Neuroimaging Biomarkers Predict Brain Structural Connectivity Change in a Mouse Model of Vascular Cognitive Impairment

Philipp Boehm-Sturm, PhD*; Martina Füchtemeier, PhD*; Marco Foddis; Susanne Mueller;
Rebecca C. Trueman, PhD; Marietta Zille, PhD; Jan Leo Rinnenthal, PhD;
Theodore Kypraios, PhD; Laurence Shaw, PhD; Ulrich Dirnagl, MD; Tracy D. Farr, PhD

Background and Purpose—Chronic hypoperfusion in the mouse brain has been suggested to mimic aspects of vascular cognitive impairment, such as white matter damage. Although this model has attracted attention, our group has struggled to generate a reliable cognitive and pathological phenotype. This study aimed to identify neuroimaging biomarkers of brain pathology in aged, more severely hypoperfused mice.

Methods—We used magnetic resonance imaging to characterize brain degeneration in mice hypoperfused by refining the surgical procedure to use the smallest reported diameter microcoils (160 μm).

Results—Acute cerebral blood flow decreases were observed in the hypoperfused group that recovered over 1 month and coincided with arterial remodeling. Increasing hypoperfusion resulted in a reduction in spatial learning abilities in the water maze that has not been previously reported. We were unable to observe severe white matter damage with histology, but a novel approach to analyze diffusion tensor imaging data, graph theory, revealed substantial reorganization of the hypoperfused brain network. A logistic regression model from the data revealed that 3 network parameters were particularly efficient at predicting group membership (global and local efficiency and degrees), and clustering coefficient was correlated with performance in the water maze.

Conclusions—Overall, these findings suggest that, despite the autoregulatory abilities of the mouse brain to compensate for a sudden decrease in blood flow, there is evidence of change in the brain networks that can be used as neuroimaging biomarkers to predict outcome. (*Stroke*. 2017;48:468-475. DOI: 10.1161/STROKEAHA.116.014394.)

Key Words: biomarkers ∎ diffusion tensor imaging ∎ hypoperfusion ∎ magnetic resonance imaging ∎ mouse ∎ neuroimaging ∎ vascular cognitive impairment

Vascular risk factors are thought to be the pathological initiation point in the development of vascular cognitive impairment.[1] There are many vascular cognitive impairment subtypes with a variety of radiological features ranging from microbleeds and lacunar infarctions to diffuse white matter hyperintensities. Progression of white matter hyperintensities is highly predictive of cognitive decline.[2] The mouse model of bilateral carotid artery stenosis attracted attention when the authors reported rarefaction and degeneration of the corpus callosum after 30 days of brain hypoperfusion.[3] A follow-up study reported that hypoperfused mice exhibited cognitive deficits, specifically spatial working memory impairments in the radial arm maze.[4] Similar deficits were reported using the same model, but with a more subtle pathology that instead includes small accumulations of degraded myelin basic protein and a change in the distribution of myelin-associated glycoprotein in several white matter structures.[5] Another group has observed a loss of fluoromyelin staining and an increase in matrix metalloproteinase-9 in the corpus callosum of hypoperfused mice, which can be prevented with free radical scavengers.[6,7] Whether or not this range of pathological changes are detectable with neuroimaging is less clear. Decreases in fractional anisotropy (FA), using diffusion tensor imaging (DTI), were observed in white matter,[8] which became more

pronounced with 6 months of hypoperfusion.[9] Our group has failed to observe FA decreases in hypoperfused mice, though we have reported alterations in several other quantitative DTI parameters.[10] In our hands, this model has been both behaviorally and histologically mild, which might reflect inherent variability of the model, or the fact that rodents exhibit a high degree of recovery and compensation. Therefore, the purpose of this study was 2-fold. First, we aimed to increase the severity of hypoperfusion using a refined surgical approach in aged mice, to improve the phenotype. Second, we aimed to identify neuroimaging biomarkers of degeneration with focus on graph theory to our DTI data to predict cognitive decline.

Methods

Experiments were approved by the Landesamt für Gesundheit und Soziales and conducted according to the German Animal Welfare Act and institutional guidelines. Twenty-four male C57/BL6 J mice (purchased at 8 weeks of age, Charles River, Germany) were housed in a temperature (22±2°C), humidity (55±10%), and light (12/12-hour light/dark cycle) controlled environment. Unexpectedly, 1 animal needed to be humanely euthanized before randomization in accordance with our animal permissions because of ill health and substantial weight loss. The remaining animals were later randomized between 9 and 13 months of age to undergo hypoperfusion (n=12) or sham (n=11). Hypoperfusion was induced by winding a custom ordered, nonmagnetic, surgical grade microcoil (160 μm inner diameter; Shannon Coiled Springs Microcoil, Limerick, Ireland) around one of the carotid arteries. The sham procedure was performed with a larger diameter microcoil (500 μm) that did not constrict the vessel. The muscles and glands were guided back into place, and local anesthetic was applied to the sutured wound before recovery. Twenty-four hours later, the same procedure was repeated on the other carotid artery. This delay represents an important refinement that does not result in higher mortality when using the smaller sized microcoils. All experimenters were blind, and all analysis was performed blind. Mice were imaged before and at 24 hours and 1- and 4-weeks post-surgery for estimation of cerebral blood flow (CBF) using arterial spin labeling. DTI, magnetic resonance spectroscopy, and angiography were acquired between 5- and 7-weeks post-surgery. The novel object recognition test was conducted 1 week before and between 4- and 5-weeks post-surgery. At 6 weeks, animals were trained in the Morris water maze, and tissue was processed for immunohistochemistry. Detailed methods are available in the online-only Data Supplement.

Results

Deficits in CBF After Hypoperfusion Recover and Are Accompanied by Changes in the Cerebrovasculature and Hippocampal Degeneration

CBF remained stable across all time points in the sham group but decreased by more than half within 24 hours of surgery in the hypoperfused group. Within 1 week, CBF began to increase in the hypoperfused group; it continued to increase but was still significantly different from shams at 4 weeks (Figure 1A and 1B, main effect of time $F_{(2.3,43.3)}10.212$; $P=0.0001$; and group $F_{(1,19)}36.977$; $P=0.0001$; and interaction $F_{(2.3,43.3)}10.240$; $P=0.0001$). This suggests that the hypoperfused mouse brain is autoregulating in response to a decrease in CBF. Angiography at 7 weeks (Figure 1A) revealed increased tortuosity in the Circle of Willis, which may be partially responsible for the recovery in CBF. However, the overall size of the Circle of Willis vasculature was not significantly different between groups (Figure IA in the online-only Data Supplement). There was no
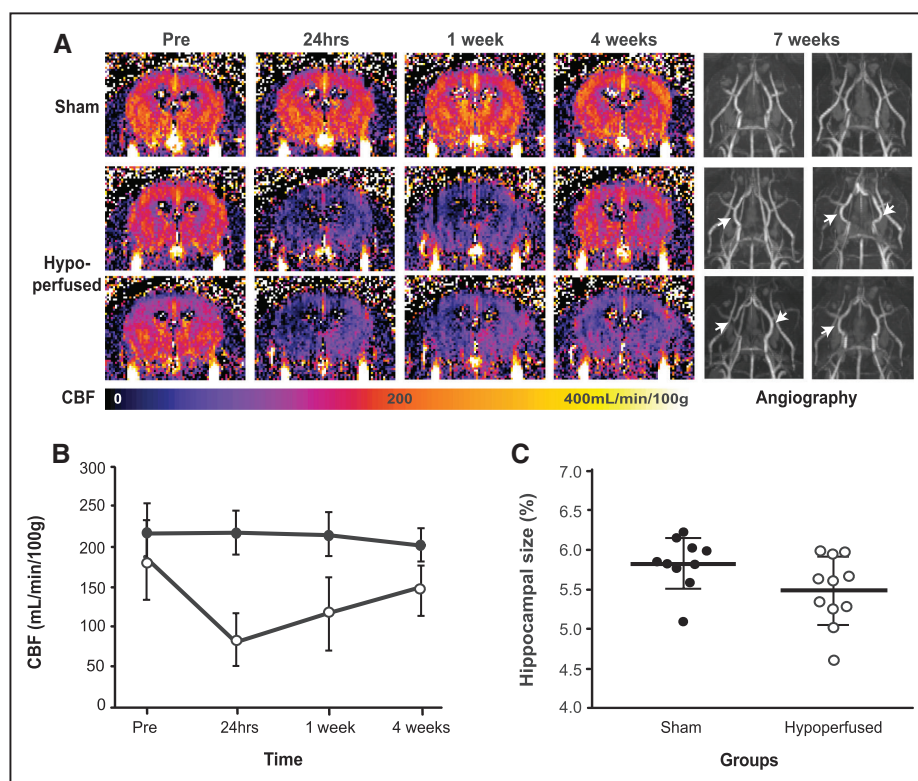

Figure 1. Cerebral blood flow (CBF) and morphological changes in the hypoperfused brain. **A**, Representative CBF maps and angiography reconstructions showing increases in Circle of Willis tortuosity in hypoperfused mice. **B**, CBF over time (means±SD) in sham (n=10) and hypoperfused (n=11) groups. **C**, % hippocampal size in both groups.
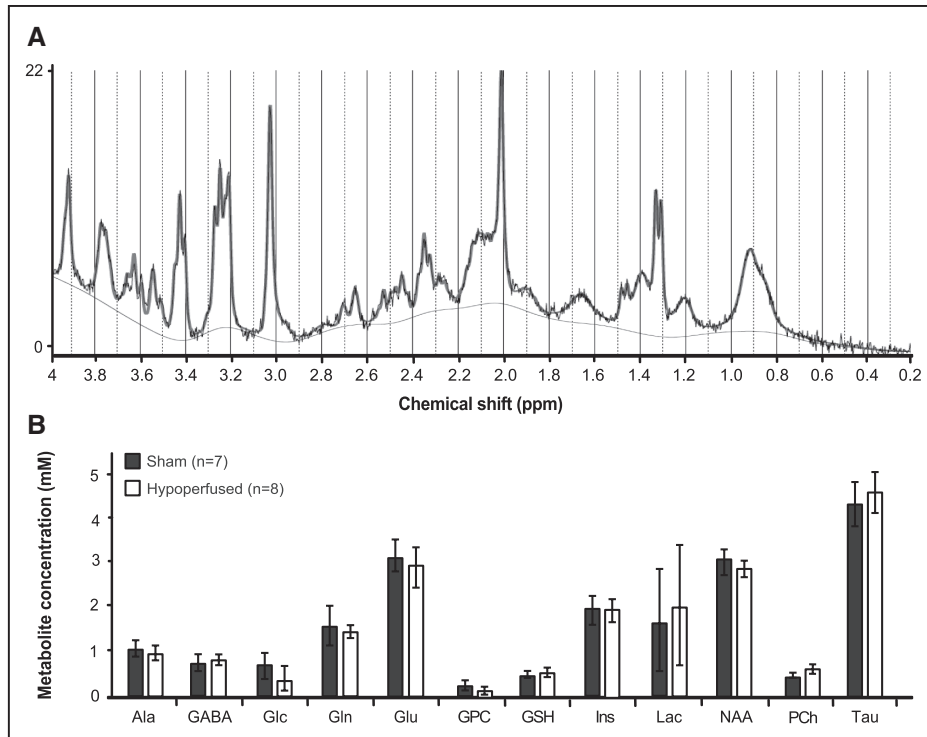
Figure 2. Brain metabolite concentrations in response to hypoperfusion. **A**, A representative spectrum from the striatum of a hypoperfused mouse. **B**, Metabolite concentrations (mmol/L) from sham and hypoperfused mice (means±SD). Ala indicates alanine; GABA, γ-aminobutyric acid; Glc, glucose; Gln, glutamine; Glu, glutamate; GPC, glycerophosphocholine; GSH, glutathione; Ins, myo-inositol; Lac, lactate (sham [n=5] and hypoperfused [n=6]); NAA, N-acetylaspartate; PCh, phosphocholine; and Tau, taurine.

significant difference in ventricle:brain ratio (Figure IB in the online-only Data Supplement), but there was a decrease in hippocampal size in the hypoperfused mice, though this failed to achieve significance (Figure 1C; Student unpaired t test t(19)2.068; P=0.053).

Metabolite concentrations were measured in the striatum with magnetic resonance spectroscopy (Figure 2), but there were no significant concentration differences in any of the metabolites (Figure 2B).

Hypoperfused Brain Exhibits Little Evidence of Pathology With Diffusion Index Measures but Undergoes Substantial Network Reorganization

Seven of the 23 brain regions from the DTI data were selected for analysis: anterior commissure, corpus callosum, and internal capsule, as well as gray matter that may be affected by hypoperfusion or is presumed to be involved in cognitive decline: hippocampus, striatum, cingulate cortex, and thalamus. FA, mean diffusivity, axial diffusivity, and radial diffusivity values are depicted for both groups in 2 white and 1 gray matter structure (Figure 3A through 3D). FA and axial diffusivity decreases are correlated with tissue degeneration and axonal degradation, whereas mean diffusivity and radial diffusivity increases are correlated with loss of tissue integrity and demyelination.[11] There were no significant differences between groups in any of the structures, suggesting little damage to the white matter.

Despite this, the reconstructed corpus callosum seemed reduced in hypoperfused mice (Figure 4). Graph theory integrated all the DTI trajectories and identified changes at a

network level. There were no significant differences between groups for global efficiency (Figure 4A), suggesting that the overall ability of the brain network to exchange information was minimally affected by hypoperfusion. However, significant group differences were noted in several measures of functional segregation. Modularity was significantly lower in the hypoperfused group (Student unpaired t test t(17)3.028; P=0.014; Figure 4B), which suggests a reduced number of heavily interconnected subgroups of structures. Interestingly, several lower level clustering parameters were significantly higher in the hypoperfused group: transitivity (Student unpaired t test: t(17)-4.706; P=0.0007; Figure 4C), clustering coefficient (Mann–Whitney U test: U=9, z=−2.939; P=0.007; Figure IIA in the online-only Data Supplement), and local efficiency (Student unpaired t test: t(17)-3.410; P=0.007; Figure 4D). These 3 parameters were also highly correlated. Transitivity and clustering coefficient rely on the presence of triangles (groups of 3 connected brain structures). This reflects an increase in the total number of connected triplets, as well as the prevalence of clustering in general and an increased ability of small subnetworks to function when any given node is removed. No significant differences were noted for degrees or assortativity (Figure IIB and IIC in the online-only Data Supplement).

A logistic regression model from the network parameters was fitted to the data. The response variable was group classification, and the covariates were the different network parameters. We performed model selection by exploring all possible models and chose the 1 with the minimum Akaike Information Criterion, which penalizes models with too many parameters.
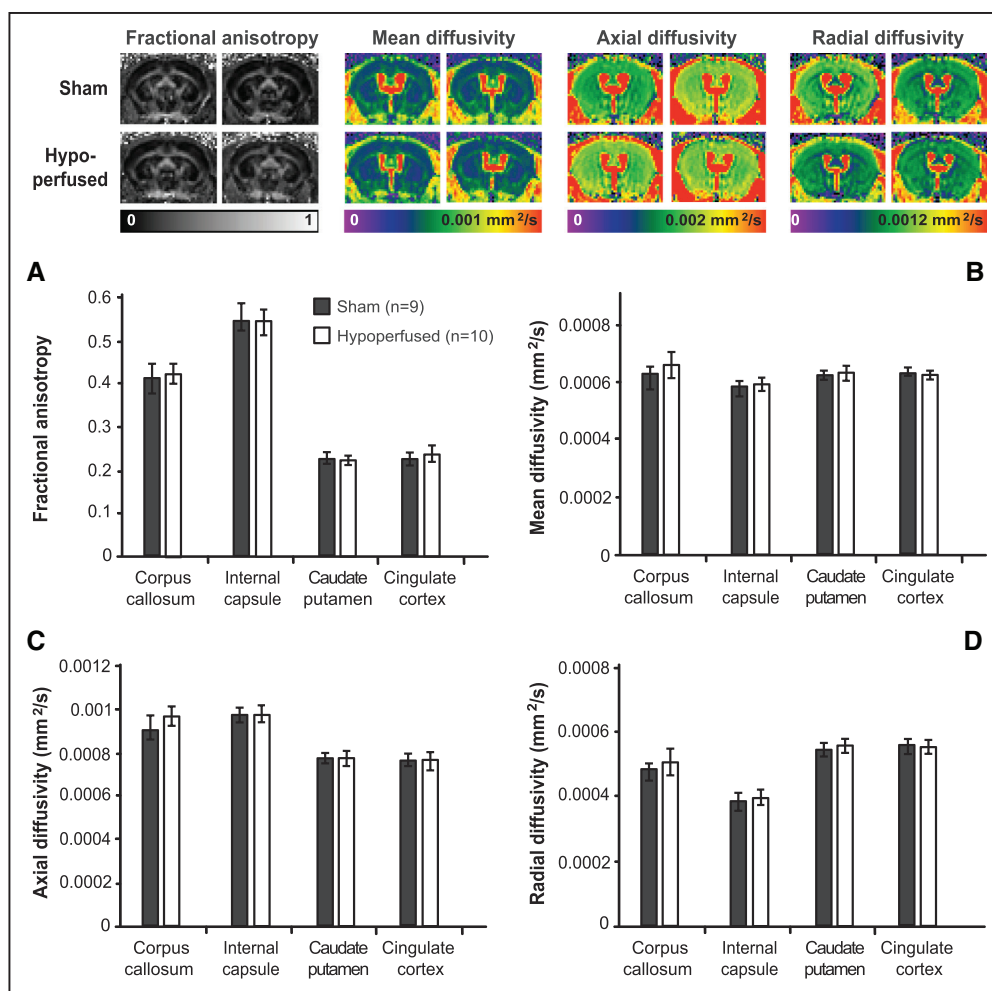
Figure 3. The effects of hypoperfusion on diffusion tensor imaging (DTI) indices. Quantitative fractional anisotropy (FA), mean diffusivity (MD), axial diffusivity (AD), and radial diffusivity (RD) maps from 2 representative animals per group (calibration bars correspond to quantitative values). **A**, FA; (**B**) MD; (**C**) AD; and (**D**) RD (means±SD) in both groups.

The best model showed that global and local efficiency and degrees could accurately classify the 2 groups of mice. Cross validation (by removing one animal at a time) showed that 15 of 19 animals were still correctly classified.

Reactive Gliosis Was Observed in the Hippocampus of Some Hypoperfused Mice Without Overt Rarefaction of the White Matter

We observed no evidence of white matter rarefaction with Luxol blue stain (Figure 5). There was also no evidence of increased astrocytic or microglial activity in any of the white matter structures. However, there was some reactive gliosis and scarring in the hippocampus of 2 of the hypoperfused mice.

Hypoperfusion Reduces Spatial Learning in the Water Maze, and Performance Is Correlated With Network Analysis Measures

Escape latencies decreased over the testing period (Figure 6A, main effect of time $F(3.9,80)13.2$; $P=0.0001$), and mice travelled decreasing distances to the platform (Figure IIIA in the online-only Data Supplement; main effect of time $F(6,108)16.1$; $P=0.0001$), indicating that both groups acquired the paradigm. However, hypoperfused mice exhibited slightly longer escape latencies than shams (Figure 6A, main effect of group $F(1,18)6.6$; $P=0.01$) and travelled greater distances to find the platform (main effect of group $F(1,18)4.7$; $P=0.04$), indicating a reduced rate of learning. There were no significant differences in swim speeds between groups (Figure 6B, no main effect of time $F(3.17,57.183)0.709$; $P=0.558$ or group $F(1,18)1.049$; $P=0.319$), suggesting that motor function was intact. There were no significant differences in the time spent in the target quadrant during the probe trial (Figure IIIB in the online-only Data Supplement). Furthermore, overall performance across the 7 days in the water maze was correlated with several network parameters: degrees, global and local efficiency, and clustering coefficient (Pearson correlation coefficients of 0.052, 0.282, 0.285, and 0.364; $P=0.069$).

During the first trial in the novel object recognition test, discrimination ratios were ≈0.5, indicating that both groups explored the 2 objects equally. This occurred both before surgery (0.49±0.03 [sham] and 0.53±0.07 [hypoperfused]) and at 4-weeks post-surgery (0.55±0.1 [sham] and 0.59±0.1 [hypoperfused]). Discrimination ratios increased during the second trial (values >0.5=greater novel object exploration), indicating biased exploration of the novel object (Figure 6C). The
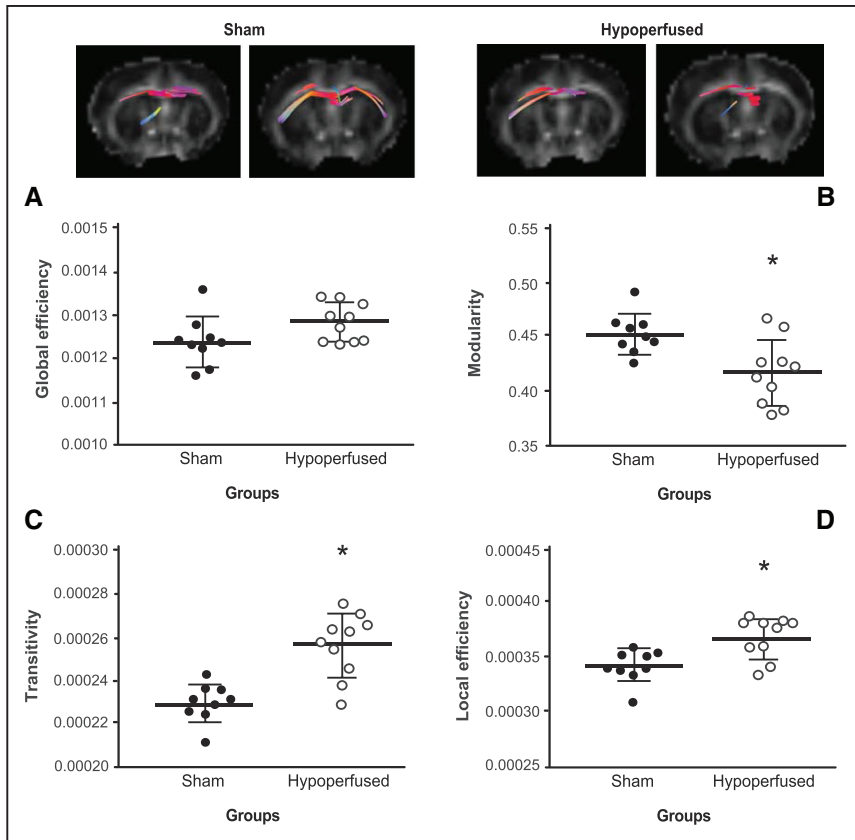
Figure 4. Graph theory revealed microstructural network changes in the hypoperfused brain. Representative reconstructions of the corpus callosum from 2 animals in each group. **A**, Global efficiency; (**B**) modularity, (**C**) transitivity, and (**D**) local efficiency in both groups.

mean discrimination ratio of shams increased at 4 weeks and decreased in the hypoperfused group when compared with baseline. However, there was no significant effect of time or group (Figure 6C; $F_{(1,17)}0.0001$; $P=0.983$ and $F_{(1,17)}0.5$; $P=0.48$, respectively). This might reflect excessive exposure over time to the testing environment. For example, discrimination ratios on the second trial varied widely at 4 weeks (Figure 6C) because some animals explored very little (1 sham animal performed no exploration [data entered as missing]). Indeed, overall % time exploring the objects decreased in both groups at 4 weeks (5.6±1.4 [sham] and 4.7±1.2 [hypoperfused]) when compared with baseline (7.5±1.2 [sham] and 8.2±2.6 [hypoperfused]). When combined, exploration time was significantly lower at 4 weeks (Student paired t test t(19)4.0; $P=0.001$).

Discussion

This study demonstrates that CBF increases with time in this mouse model of hypoperfusion, which may be because of increases in tortuosity of the Circle of Willis. Although no brain atrophy was observed (ventricle:brain ratio), there was hippocampal shrinkage in the hypoperfused mice and reactive astrogliosis in the hippocampus of 2 mice. This was combined with spatial learning impairments in the water maze. We did not observe white matter rarefaction in the hypoperfused animals with basic histology, though this is
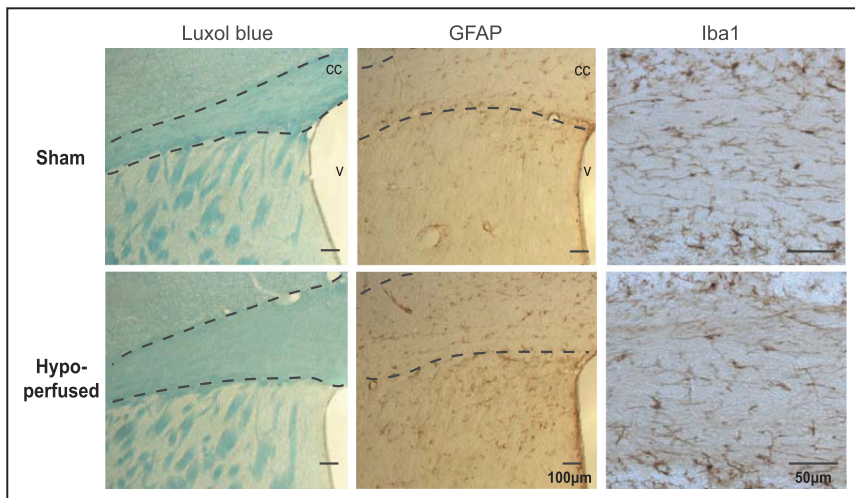

Figure 5. White matter integrity and astrogliosis in the hypoperfused brain. Luxol blue, GFAP, and Iba1 stained tissue sections from the corpus callosum of a representative animal in each group (dotted line outlines the corpus callosum [cc]. v indicates ventricles.
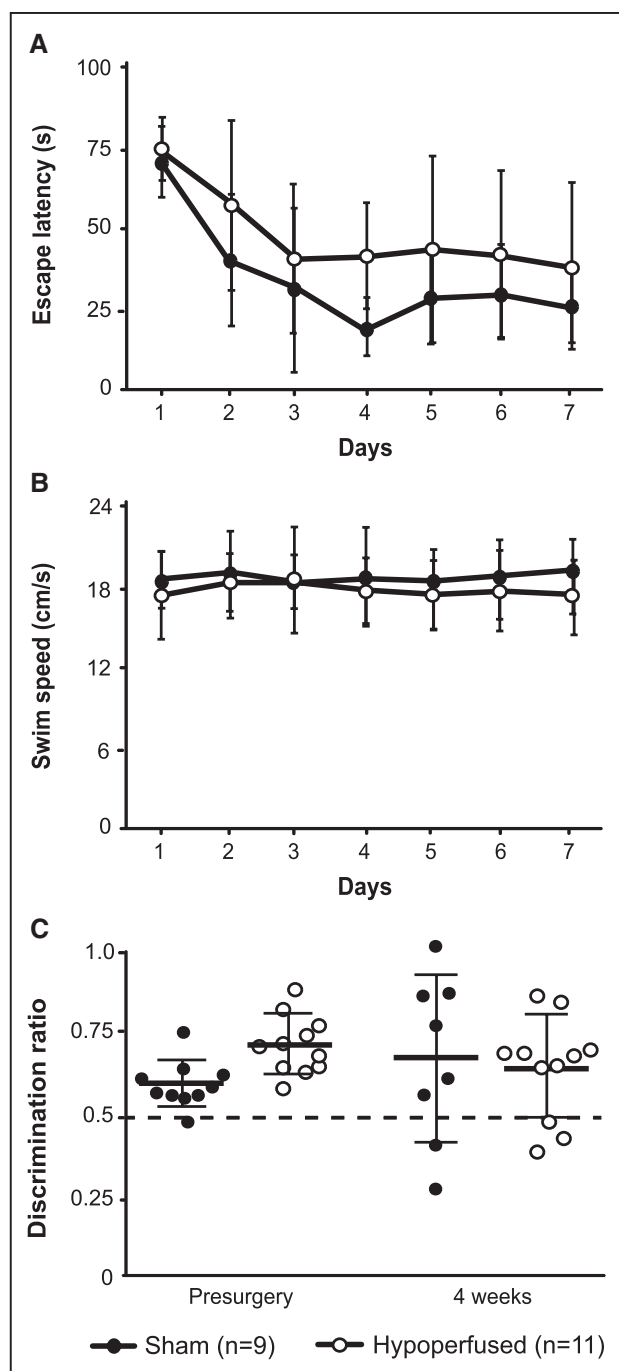
Figure 6. The effects of hypoperfusion on spatial learning and short-term recognition memory. **A**, Escape latency and (**B**) swim speed of both groups during the Morris water maze place task (means±SD). **C**, Discrimination ratio of both groups in the second trial of the novel object recognition (NOR) task before and at 4-wk post-surgery (>0.5 indicates increased exploration of the novel object).

not surprising, because the pathology has been reported to be more subtle. The hypoperfused brain had clearly reorganized because application of graph theory to structural connectivity data showed an overall reduction in the ability to subdivide the brain into distinctive groups of highly interconnected structures, combined with an increase in connectivity among clusters of brain structures. Some network parameters were

correlated with water maze deficits, and others were excellent predictors of outcome.

We reported a decrease in CBF that increases with time that was comparable to our previous results,[10] as well as findings from the article that introduced this model: CBF recovered to within 10% of presurgical levels by 30 days.[3] Similar results have also been reported with CBF recovery to 81.7% at 1 month[12] and to 80% as early as 14 days after hypoperfusion.[13] All of the previous studies used 180-μm-diameter microcoils made from piano wire. We have found that this material dissolves after implantation (Figure IV in the online-only Data Supplement) and could have explained the CBF recovery reported in these studies. However, the present study used a smaller diameter microcoil (160 μm) made from nonmagnetic, surgical grade material that was recovered at the conclusion of the experiments (Figure IV in the online-only Data Supplement), and near recovery of CBF was still observed in the hypoperfused group that occurred to a lesser extent than when 180 μm coils were used (Figure V in the online-only Data Supplement). We observed increases in the tortuosity of the Circle of Willis with angiography that may be partially responsible for the recovery in CBF because this collateral structure attempts to compensate. We did not observe an increase in Circle of Willis size; therefore, we hesitate to conclude that tortuosity equals arteriogenesis, though it is possible this phenomenon is playing a role in the observed CBF increase. We also substantially reduced interindividual variation and confirmed no changes in sham CBF, by using nonmagnetic microcoils in this study. At least when using magnetic resonance imaging, this strategy is necessary because the magnetic microcoils made from piano wire compromise CBF measurements by interfering with the magnetic resonance imaging acquisition.

Spatial working memory impairments have been reported in hypoperfused mice in the radial arm maze; animals displayed an increase in the number of revisiting errors after 1[4,5] and 8 months of hypoperfusion.[12] Spatial learning deficits in the water maze had not been previously observed until hypoperfusion was extended to 6 months.[9] Compared with this, we increased the severity of hypoperfusion and thus may have achieved deficits sooner. Consistent with the prevailing hypothesis, it is possible that these memory deficits are because of white matter damage. However, it is also possible that the deficits are because of hippocampal damage. We observed a nonsignificant decrease in hippocampal size in this model, along with reactive astrogliosis in 2 hypoperfused mice. This is in line with 1 report that observed this in the most severely deprived hemisphere (with 160 μm inner diameter microcoils) when the degree of hypoperfusion was varied.[14] Other groups have reported hippocampal damage after hypoperfusion.[12,15,16] Working memory in the radial arm and water maze has a strong spatial component that is particularly sensitive to hippocampal damage. We chose the novel object recognition task to avoid this as much as possible; this task requires intact perirhinal and prefrontal cortices.[17,18] There was decreased novel object exploration in the hypoperfused mice after 4 weeks when compared with baseline, but this was not significant. We did observe high variability in overall exploration at 4 weeks (compared with baseline) that we think is because of mice being overly habituated to the test environment; indeed, they spent less time exploring the objects in

general after the second exposure. In the future, we will avoid repeated exposure to this test.

In this experiment, we were unable to detect white matter change using DTI indices, despite previously reporting increases in mean diffusivity, radial diffusivity, and axial diffusivity (but no change in FA) in several brain structures.[10] Another group has shown decreases in FA in the corpus callosum and internal capsule of hypoperfused mice after 1 and 6 months, with no corresponding changes in mean diffusivity.[8,9] It is possible that our automated analysis strategy may have contributed to the lack of effects. Despite making substantial effort to modify the atlas to reflect our DTI data, smaller structures, such as the corpus callosum, did not consistently coregister well. Basic histology was also performed to look for gross changes in the white matter, and, in support of the DTI index data, white matter rarefaction was not observed. It is likely that the pathology associated with the white matter was too subtle to be detected with either DTI indices or Luxol blue. Indeed, the white matter rarefaction reported in the original studies[3,4] has not been replicated by ourselves[10,15] or others.[5,8,9] The latter studies report a more subtle pathology that is consistent with hypoxic disruption of myelin integrity in the white matter structures. There were small accumulations of myelin debris (degraded myelin basic protein), and myelin-associated glycoprotein staining took on a discontinuous and granular appearance. Another study has reported that, although myelin-associated glycoprotein protein levels do not change, the granular myelin-associated glycoprotein reflects a loss of cellular distribution that is likely associated with disruption in axon–glia interactions.[19] One potential limitation of the present study is that the mice were trained in 9 hole boxes; though they failed to reach criteria, it is possible that this acted as a form of enrichment and protected them against the more severe hypoperfusion procedure. Indeed, we have observed a more pronounced phenotype when the smaller (160 μm) microcoils were implanted into naïve mice.

Graph theory is a popular mathematical technique that models the complex organization of the brain. It is a novel approach for studying structural and functional human brain connectivity with neuroimaging techniques and is gaining popularity as a way to understand the diseased brain.[20,21] There are a few recent reports that examine connectomes of the intact rodent brain.[22,23] We are among the first to apply this technique to mouse brain DTI data and the first to detect changes in the hypoperfused brain. Global efficiency is a well-defined measure reflecting the potential for functional integration of information.[24] It is strongly related to the density of connections, and decreases are accepted as a marker of network deterioration. A decline in global efficiency has predicted the development of dementia in patients with small vessel disease.[25] Although we failed to observe a group difference in this study, global efficiency was extremely reproducible and, along with local efficiency and degrees, was successfully able to classify our groups using the logistic regression model; therefore, it is a valuable biomarker for hypoperfusion. Measures of functional segregation refer to the existence of subnetworks composed of structures that are heavily interconnected and thus presumed to participate in specialized functions. Modularity is strongly related to the adaptability of a system and was significantly decreased in the hypoperfused group. This indicates fewer distinctive subnetworks. Local efficiency estimates how well a local subnetwork is connected to any particular structure. Interestingly, we observed an increase in local efficiency in the hypoperfused group, alongside an increase in clustering coefficient and transitivity (other measures of connectivity within smaller subnetworks of 3 regions). Similar increases have been reported in patients with small vessel disease, which were negatively correlated with cognitive performance, and interpreted as small changes in tissue microstructure within particular hubs.[26] It is possible the results of this study may reflect some degree of compensation on the part of the hypoperfused brain: closely connected structures increase their connections in response to an overall decline in the connections between larger functional subnetworks. One limitation of this type of analysis is that it is highly dependent on the number and density of connections. However, there was no difference in the number of connections between groups. The lack of atrophy in the hypoperfused mice would also suggest that our results are biologically meaningful, despite not being fully explained. It is also possible that with a larger sample size, or a greater amount of data as this technique becomes more prevalent, we could validate the model. The hypertensive rat has been suggested as another animal model of vascular cognitive impairment because it exhibits recognition memory deficits and reduced white matter integrity without overt white matter lesions.[27] Graph theory has been recently pioneered in the spontaneously hypertensive rat and revealed a decrease in global and local efficiency and modularity.[28] This suggests an overall decline in functional integration and segregation in the spontaneously hypertensive rat, as opposed to the reorganization of subnetworks we observed in the hypoperfused mouse. More studies that use this type of analysis are necessary to improve our understanding of how the different types of pathologies correlate with network alterations. It should also be cautioned that differences in acquisition parameters and postprocessing strategies, particularly tractography methods, can produce different results, and this should always be carefully considered. It has also been suggested that generative network models, such as exponential graph models, might be a useful alternative to the descriptive work presented here.[29]

Our strategy to use aged mice and increase the severity of hypoperfusion resulted in a more reproducible phenotype because subtle behavioral impairments were observed. We also successfully identified several novel neuroimaging biomarkers for use with this mouse model. Accurate CBF imaging can be used to stratify groups of mice, and DTI in particular provided several quantitative indices alongside useful network parameters that were accurately able to predict outcome.

Sources of Funding

Disclosures

None.

References

1. Iadecola C. The pathobiology of vascular dementia. *Neuron*. 2013;80:844–866. doi: 10.1016/j.neuron.2013.10.008.

2. Jokinen H, Schmidt R, Ropele S, Fazekas F, Gouw AA, Barkhof F, et al; LADIS Study Group. Diffusion changes predict cognitive and functional outcome: the LADIS study. *Ann Neurol*. 2013;73:576–583. doi: 10.1002/ana.23802.

3. Shibata M, Ohtani R, Ihara M, Tomimoto H. White matter lesions and glial activation in a novel mouse model of chronic cerebral hypoperfusion. *Stroke*. 2004;35:2598–2603. doi: 10.1161/01. STR.0000143725.19053.60.

4. Shibata M, Yamasaki N, Miyakawa T, Kalaria RN, Fujita Y, Ohtani R, et al. Selective impairment of working memory in a mouse model of chronic cerebral hypoperfusion. *Stroke*. 2007;38:2826–2832. doi: 10.1161/STROKEAHA.107.490151.

5. Coltman R, Spain A, Tsenkina Y, Fowler JH, Smith J, Scullion G, et al. Selective white matter pathology induces a specific impairment in spatial working memory. *Neurobiol Aging*. 2011;32:2324.e7–2324.e12. doi: 10.1016/j.neurobiolaging.2010.09.005.

6. Seo JH, Miyamoto N, Hayakawa K, Pham LD, Maki T, Ayata C, et al. Oligodendrocyte precursors induce early blood-brain barrier opening after white matter injury. *J Clin Invest*. 2013;123:782–786. doi: 10.1172/JCI65863.

7. Miyamoto N, Maki T, Pham LD, Hayakawa K, Seo JH, Mandeville ET, et al. Oxidative stress interferes with white matter renewal after prolonged cerebral hypoperfusion in mice. *Stroke*. 2013;44:3516–3521. doi: 10.1161/STROKEAHA.113.002813.

8. Holland PR, Bastin ME, Jansen MA, Merrifield GD, Coltman RB, Scott F, et al. MRI is a sensitive marker of subtle white matter pathology in hypoperfused mice. *Neurobiol Aging*. 2011;32:2325.e1–2325.e6. doi: 10.1016/j.neurobiolaging.2010.11.009.

9. Holland PR, Searcy JL, Salvadores N, Scullion G, Chen G, Lawson G, et al. Gliovascular disruption and cognitive deficits in a mouse model with features of small vessel disease. *J Cereb Blood Flow Metab*. 2015;35:1005–1014. doi: 10.1038/jcbfm.2015.12.

10. Füchtemeier M, Brinckmann MP, Foddis M, Kunz A, Po C, Curato C, et al. Vascular change and opposing effects of the angiotensin type 2 receptor in a mouse model of vascular cognitive impairment. *J Cereb Blood Flow Metab*. 2015;35:476–484. doi: 10.1038/jcbfm.2014.221.

11. Alexander AL, Lee JE, Lazar M, Field AS. Diffusion tensor imaging of the brain. *Neurotherapeutics*. 2007;4:316–329. doi: 10.1016/j.nurt.2007.05.011.

12. Nishio K, Ihara M, Yamasaki N, Kalaria RN, Maki T, Fujita Y, et al. A mouse model characterizing features of vascular dementia with hippocampal atrophy. *Stroke*. 2010;41:1278–1284. doi: 10.1161/STROKEAHA.110.581686.

13. Hattori Y, Enmi J, Kitamura A, Yamamoto Y, Saito S, Takahashi Y, et al. A novel mouse model of subcortical infarcts with dementia. *J Neurosci*. 2015;35:3915–3928. doi: 10.1523/JNEUROSCI.3970-14.2015.

14. Miki K, Ishibashi S, Sun L, Xu H, Ohashi W, Kuroiwa T, et al. Intensity of chronic cerebral hypoperfusion determines white/gray matter injury and cognitive/motor dysfunction in mice. *J Neurosci Res*. 2009;87:1270–1281. doi: 10.1002/jnr.21925.

15. Jadavji NM, Farr TD, Lips J, Khalil AA, Boehm-Sturm P, Foddis M, et al. Elevated levels of plasma homocysteine, deficiencies in dietary folic acid and uracil-DNA glycosylase impair learning in a mouse model of vascular cognitive impairment. *Behav Brain Res*. 2015;283:215–226. doi: 10.1016/j.bbr.2015.01.040.

16. Zuloaga KL, Zhang W, Yeiser LA, Stewart B, Kukino A, Nie X, et al. Neurobehavioral and imaging correlates of hippocampal atrophy in a mouse model of vascular cognitive impairment. *Transl Stroke Res*. 2015;6:390–398. doi: 10.1007/s12975-015-0412-z.

17. Barker GR, Warburton EC. When is the hippocampus involved in recognition memory? *J Neurosci*. 2011;31:10721–10731. doi: 10.1523/JNEUROSCI.6413-10.2011.

18. Akirav I, Maroun M. Ventromedial prefrontal cortex is obligatory for consolidation and reconsolidation of object recognition memory. *Cereb Cortex*. 2006;16:1759–1765. doi: 10.1093/cercor/bhj114.

19. Reimer MM, McQueen J, Searcy L, Scullion G, Zonta B, Desmazieres A, et al. Rapid disruption of axon-glial integrity in response to mild cerebral hypoperfusion. *J Neurosci*. 2011;31:18185–18194. doi: 10.1523/JNEUROSCI.4936-11.2011.

20. Chen G, Zhang HY, Xie C, Chen G, Zhang ZJ, Teng GJ, et al. Modular reorganization of brain resting state networks and its independent validation in Alzheimer's disease patients. *Front Hum Neurosci*. 2013;7:456. doi: 10.3389/fnhum.2013.00456.

21. Iturria-Medina Y. Anatomical brain networks on the prediction of abnormal brain states. *Brain Connect*. 2013;3:1–21. doi: 10.1089/brain.2012.0122.

22. Stafford JM, Jarrett BR, Miranda-Dominguez O, Mills BD, Cain N, Mihalas S, et al. Large-scale topology and the default mode network in the mouse connectome. *Proc Natl Acad Sci USA*. 2014;111:18745–18750. doi: 10.1073/pnas.1404346111.

23. Liska A, Galbusera A, Schwarz AJ, Gozzi A. Functional connectivity hubs of the mouse brain. *Neuroimage*. 2015;115:281–291. doi: 10.1016/j.neuroimage.2015.04.033.

24. Rubinov M, Sporns O. Complex network measures of brain connectivity: uses and interpretations. *Neuroimage*. 2010;52:1059–1069. doi: 10.1016/j.neuroimage.2009.10.003.

25. Tuladhar AM, van Uden IW, Rutten-Jacobs LC, Lawrence A, van der Holst H, van Norden A, et al. Structural network efficiency predicts conversion to dementia. *Neurology*. 2016;86:1112–1119. doi: 10.1212/WNL.0000000000002502.

26. Kim HJ, Im K, Kwon H, Lee JM, Ye BS, Kim YJ, et al. Effects of amyloid and small vessel disease on white matter network disruption. *J Alzheimers Dis*. 2015;44:963–975. doi: 10.3233/JAD-141623.

27. Kaiser D, Weise G, Möller K, Scheibe J, Pösel C, Baasch S, et al. Spontaneous white matter damage, cognitive decline and neuroinflammation in middle-aged hypertensive rats: an animal model of early-stage cerebral small vessel disease. *Acta Neuropathol Commun*. 2014;2:169. doi: 10.1186/s40478-014-0169-8.

28. López-Gil X, Amat-Roldan I, Tudela R, Castañé A, Prats-Galino A, Planas AM, et al. DWI and complex brain network analysis predicts vascular cognitive impairment in spontaneous hypertensive rats undergoing executive function tests. *Front Aging Neurosci*. 2014;6:167. doi: 10.3389/fnagi.2014.00167.

29. Sinke MR, Dijkhuizen RM, Caimo A, Stam CJ, Otte WM. Bayesian exponential random graph modeling of whole-brain structural networks across lifespan. *Neuroimage*. 2016;135:79–91. doi: 10.1016/j.neuroimage.2016.04.066.